

# Cinchonine, a Potential Oral Small-Molecule Glucagon-Like Peptide-1 Receptor Agonist, Lowers Blood Glucose and Ameliorates Non-Alcoholic Steatohepatitis

Huan Xue<sup>1,\*</sup>, Hao-Jie Xing<sup>1,\*</sup>, Bin Wang<sup>1</sup>, Chao Fu<sup>1</sup>, Yu-Shan Zhang<sup>1</sup>, Xi Qiao<sup>1</sup>, Chao Guo<sup>1</sup>, Xiao-Li Zhang<sup>1</sup>, Bin Hu<sup>1</sup>, Xin Zhao<sup>1</sup>, Li-Jiao Deng<sup>1</sup>, Xiao-Chan Zhu<sup>1</sup>, Yi Zhang<sup>1</sup>, Yun-Feng Liu<sup>2</sup>

<sup>1</sup>Department of Pharmacology, Shanxi Medical University, Taiyuan, 030001, People's Republic of China; <sup>2</sup>Department of Endocrinology, First Hospital of Shanxi Medical University, Shanxi Medical University, Taiyuan, 030001, People's Republic of China

\*These authors contributed equally to this work

Correspondence: Yi Zhang; Yun-Feng Liu, Tel +86-18835102847; +86-18703416169, Email yizhang313@163.com; nectarliu@163.com

**Purpose:** The glucagon-like peptide-1 receptor (GLP-1R) is an effective therapeutic target for type 2 diabetes mellitus (T2DM) and non-alcoholic steatohepatitis (NASH). Research has focused on small-molecule GLP-1R agonists because of their ease of use in oral formulations and improved patient compliance. However, no small-molecule GLP-1R agonists are currently available in the market. We aimed to screen for a potential oral small-molecule GLP-1R agonist and evaluated its effect on blood glucose and NASH.

**Methods:** The Connectivity map database was used to screen for candidate small-molecule compounds. Molecular docking was performed using SYBYL software. Rat pancreatic islets were incubated in different concentrations glucose solutions, with cinchonine or Exendin (9–39) added to determine insulin secretion levels. C57BL/6 mice, GLP-1R<sup>-/-</sup> mice and hGLP-1R mice were used to conduct oral glucose tolerance test. In addition, we fed ob/ob mice with the GAN diet to induce the NASH model. Cinchonine (50 mg/kg or 100 mg/kg) was administered orally twice daily to the mice. Serum liver enzymes were measured using biochemical analysis. Liver tissues were examined using Hematoxylin-eosin staining, Oil Red O staining and Sirius Red staining.

**Results:** Based on the small intestinal transcriptome of geniposide, a recognized small-molecule GLP-1R agonist, we identified that cinchonine exerted GLP-1R agonist-like effects. Cinchonine had a good binding affinity for GLP-1R. Cinchonine promoted glucose-dependent insulin secretion, which could be attenuated significantly by Exendin (9–39), a specific GLP-1R antagonist. Moreover, cinchonine could reduce blood glucose in C57BL/6 and hGLP-1R mice, an effect that could be inhibited with GLP-1R knockout. In addition, cinchonine reduced body weight gain and food intake in ob/ob-GAN NASH mice dose-dependently. 100 mg/kg cinchonine significantly improved liver function by reducing the ALT, ALP and LDH levels. Importantly, 100 mg/kg cinchonine ameliorated hepatic steatosis and fibrosis in NASH mice.

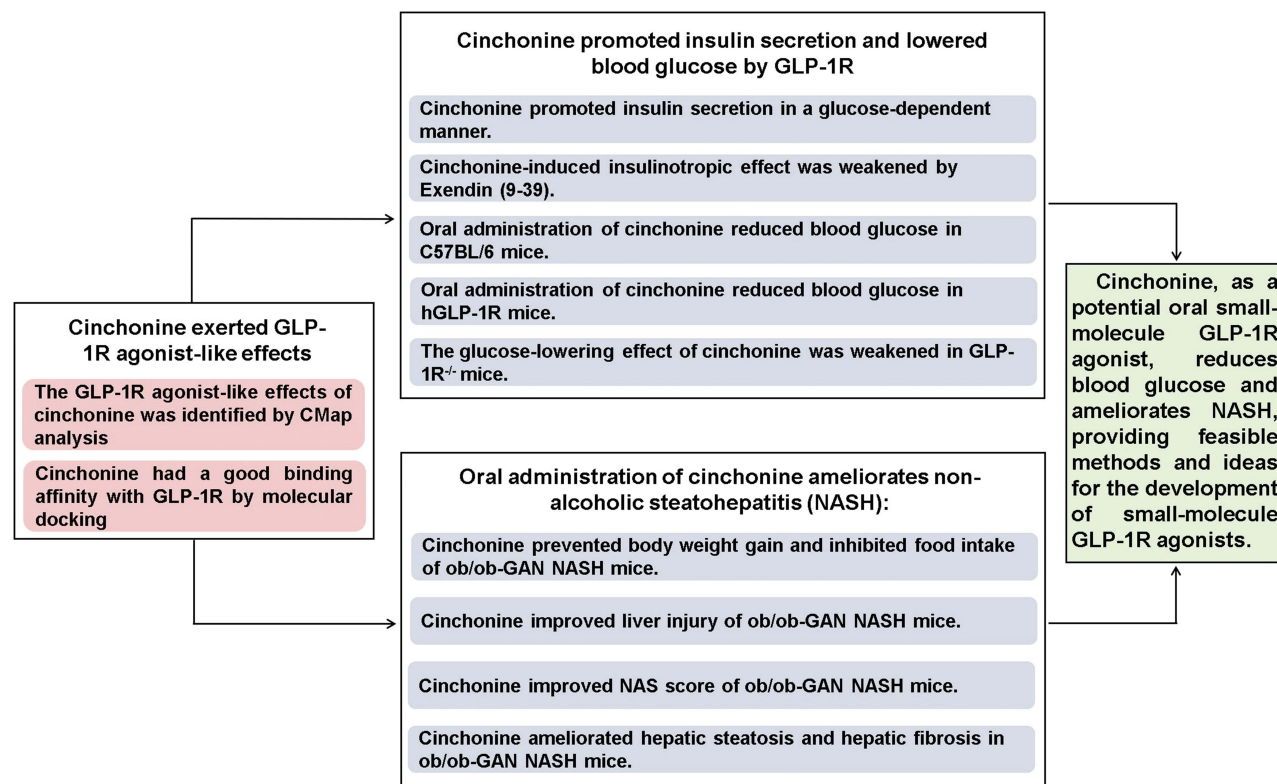
**Conclusion:** Cinchonine, a potential oral small-molecule GLP-1R agonist, could reduce blood glucose and ameliorate NASH, providing a strategy for developing small-molecule GLP-1R agonists.

**Keywords:** glucagon-like peptide-1 receptor, cinchonine, drug repurposing, non-alcoholic steatohepatitis, type 2 diabetes mellitus

## Introduction

Diabetes is a major threat to human health worldwide.<sup>1</sup> The International Diabetes Federation (IDF) has listed approximately 537 million adults with diabetes in 2021, a number expected to increase to 643 million by 2030.<sup>2</sup> Glucagon-like peptide-1 receptor (GLP-1R) agonists have shown remarkable therapeutic effects for type 2 diabetes mellitus (T2DM).<sup>3,4</sup> Furthermore, GLP-1R agonists have multiple biological effects that can treat obesity, cardiovascular, neurological, metabolic diseases and play a positive role in tumor therapy.<sup>5</sup>

## Graphical Abstract



Non-alcoholic fatty liver disease (NAFLD) ranges from simple liver steatosis at the initial stage to non-alcoholic steatohepatitis (NASH), which, if not controlled, can further develop into cirrhosis and hepatocellular cancer, seriously threatening human health.<sup>6</sup> GLP-1R agonists are important candidates for the treatment of NASH.<sup>7,8</sup> However, the clinical GLP-1R agonists are macromolecular peptide preparations.<sup>9</sup> They should be administrated by injection except for oral semaglutide, limiting their clinical application.<sup>10-12</sup> Compared to peptides, small-molecule compounds are easier to develop into oral preparations and improve patient compliance.<sup>13-15</sup> Hence, small-molecule GLP-1R agonists are highly desirable. However, no small-molecule GLP-1R agonist is available.

In recent years, the cost of traditional drug development has increased significantly. In addition, the development cycles are long and the success rate is low, which are critical factors restricting drug development.<sup>16,17</sup> Under such adverse factors, drug repurposing, namely repositioning and reevaluating marketed or investigational drugs for identifying and confirming new indications, has become an important method for drug discovery.<sup>18</sup> Connectivity Map (CMap) is a crucial tool for drug repurposing by screening compounds that can generate gene expression profiles similar to that of the target drug.<sup>19-21</sup> Currently, there is significant interest in the identification and development of nonpeptide agonists using this tool.

Here, we analyzed the small intestine transcriptome of geniposide, a recognized small-molecule GLP-1R agonist, and identified that cinchonine exerted GLP-1R agonist-like effects using CMap. Cinchonine, a quinoline alkaloid extracted from cinchona bark, has been used effectively as an antimalarial drug along with quinine, and quinidine.<sup>22</sup> It has been suggested that cinchonine is less toxic than other quinine-related compounds.<sup>23</sup> In the present study, we investigated the effect of cinchonine on hyperglycemia and NASH as a potential oral small-molecule GLP-1R agonist.

## Materials and Methods

### Animals and Drugs

Eight-week-old male BKS-Lepr<sup>em2Cd479</sup>/Gpt (db/db) mice and C57BL/6N mice were purchased from Beijing Vital River Laboratory Animal Technology Co., Ltd (Beijing, China). Six-week-old male C57BL/6 mice and adult male Wistar rats (240–260 g) were purchased from the Experimental Animal Center of the Shanxi Provincial People's Hospital (Taiyuan, China). C57BL/6N-Glp1r em1cyagen mice (GLP-1R<sup>-/-</sup> mice; KOCMP-14652-Glp1r) were purchased from Cyagen Biosciences (Suzhou, China). C57BL/6-Glp1rem2(hGLP1R) Smoc mice (hGLP-1R mice, NM-HU-200220) were obtained from Shanghai Model Organisms Center (Shanghai, China). Male B6.V-Lepob/JRj (ob/ob) mice were purchased from Cavens Experimental Center (Changzhou, China). All animals were kept in a 12 h/12 h light/dark cycle environment at 21 ± 2 °C and relative humidity of 50% ± 10%, with free access to food and water. Geniposide was obtained from Wako Pure Chemical Industries, Ltd (Osaka, Japan). Cinchonine was purchased from Topscience (Shanghai, China).

### Microarray Analysis

Eight-week-old db/db mice and C57BL/6N mice were divided into Control group (C57BL/6N mice, n=10), Model group (db/db mice, n=10) and Geniposide group (db/db mice, n=10). Mice in the Geniposide group were intraperitoneally injected with geniposide (200 mg/kg/day), while mice in the Control group and Model group were intraperitoneally injected with an identical volume of saline for 11 weeks. Three small intestine tissue samples were collected from each group for transcriptome sequencing.

Total RNA was extracted using a kit (B511311, Sangon Biotech Co., Ltd., Shanghai, China) according to the manufacturer's protocol. The quality and quantity of RNA were assessed using a Qubit<sup>®</sup> RNA Assay Kit and Qubit<sup>®</sup> 2.0 Fluorometer (Life Technologies, Carlsbad, CA, USA). High quality RNA samples were then submitted to Sangon Biotech Co., Ltd. for library preparation and sequencing using 2 µg of RNA per sample. Sequencing libraries were generated using the Hieff NGS<sup>™</sup> MaxUp Dual-mode mRNA Library Prep Kit for Illumina<sup>®</sup> (12301ES96, YEASEN Biotech Co., Ltd., Shanghai, China). To select cDNA fragments of 150–200 bp in length, the library fragments were purified with Hieff NGS<sup>™</sup> DNA Selection Beads (12601ES56, YEASEN Biotech Co., Ltd.). PCR products were purified using Hieff NGS<sup>™</sup> DNA Selection Beads and the library quality was assessed using the Qubit<sup>®</sup> 2.0 Fluorometer (Life Technologies). Paired-end sequencing of the library was performed using the Illumina<sup>®</sup> HiSeq platform (Illumina Inc., San Diego, CA, USA). For samples with biological replicates, DESeq (version 1.12.4) was used for analysis. Raw data were normalized using the robust multichip average algorithm and the limma package in R (<https://www.r-project.org>). Differentially expressed genes (DEGs) between each two groups were selected based on the following screening conditions: qValue<0.05 and |log fold-change (FC)|>1.

### Screening Candidate Small-Molecule Drugs Using CMap

The CMap database (<http://www.broadinstitute.org/cmap/>) is a credible and open website containing thousands of gene expression profiles of small-molecule compounds that act on several mammalian cells. DEGs were converted into corresponding probes using the Perl script and entered into CMap. A positive connectivity score (close to +1) indicates the compound has a gene expression profile similar to that of a specific drug. In contrast, a negative connectivity score (close to -1) indicates that the compound induces gene expression profiles opposite to that of a specific compound.<sup>24</sup>

### Molecular Docking by SYBYL Software

Molecular docking plays a crucial role in designing ligands compatible with the binding sites of macromolecules. The three-dimensional structure of cinchonine was acquired from PubChem (<https://pubchem.ncbi.nlm.nih.gov/>). The minimization of compound configuration was carried out using SYBYL.<sup>25</sup> The structure of GLP-1R (PDB ID: 5NX2) was acquired from the Protein Data Bank (<http://www.rcsb.org/pdb>). Moreover, co-crystallized ligands and water molecules were removed, whereas protons were added during protein structure preparation. The Surflex-Dock Geom X docking

mode of SYBYL was used to dock the ligand with the protein. A total score  $\geq 6$  and Cscore  $\geq 4$  was considered to indicate good affinity.

## Isolation and Culture of Rat Pancreatic Islets

Rat pancreatic islets were collected after 1 mg/mL collagenase P (Roche, Indianapolis, IN, United States) was injected into the pancreas after euthanasia and centrifuged using Histopaque<sup>TM</sup>-1077 (Sigma-Aldrich, St. Louis, MO, USA). Isolated islets were cultured in RPMI 1640 medium (Hyclone, South Logan, UT, USA) with 11.1 mM glucose (Solarbio, Beijing, China) and 10% fetal bovine serum (Gibco, Grand Island, NY, USA) supplemented with 1% penicillin and streptomycin under 37 °C and 5% CO<sub>2</sub> conditions.<sup>26</sup>

## Insulin Secretion Assay

According to the experimental design, five islets of uniform size from each group were pre-incubated in Krebs Ringer Bicarbonate-HEPES solution supplemented with 2.8 mM glucose for 30 min. Islets were then incubated in solutions of different glucose concentrations (2.8 mM, 11.1 mM, and 16.7 mM), adding cinchonine (10  $\mu$ M) or Exendin (9–39) (100 nM) (Aladdin, Shanghai, China) for 30 min. Insulin concentration was measured using a radioimmunoassay kit (North Biological Technology Research Institute, Beijing, China).

## Oral Glucose Tolerance Test (OGTT)

For OGTT, mice were fasted overnight and administered 2 g/kg glucose. Blood glucose was monitored at 0, 15, 30, 60, 90 and 120 min post glucose administration using a Sinocare glucometer (Changsha, China).<sup>27</sup> The area under the curve (AUC) for glucose was calculated for a sampling period of 0–120 min. The AUC was analyzed by Area Below Curves function of Sigmaplot software which compute the areas under multiple curves using the trapezoidal rule.

## Construction of Ob/Ob-GAN NASH Mice and Drug Intervention

C57BL/6 mice and ob/ob mice were provided free access to tap water and normal chow until they were 25-week-old. Mice were then divided into four weight-matched and liver function-matched groups (n=7 per group): NC group (C57BL/6 mice), Vehicle group (ob/ob mice), 50 mg/kg cinchonine group (ob/ob mice), and 100 mg/kg cinchonine group (ob/ob mice). Gubra Amylin NASH diet (GAN diet; D09100310, Research Diets Inc., New Brunswick, NJ, USA), containing 46% saturated fatty acids, 22% fructose, 10% sucrose, and 2% cholesterol, was obtained from Synergetic Pharmaceutical Bioengineering Company (Jiangsu, China). Cinchonine was dissolved in saline. Mice in the NC group were fed with normal chow while the other groups were fed the GAN diet. Mice in the cinchonine groups received 50 mg/kg or 100 mg/kg cinchonine by oral gavage twice a day. Mice in the NC and Vehicle groups were administered saline at the same time. Body weight and food intake were monitored daily. In addition, serum and liver tissue were collected at the end of dosing for further experiments.

## Serum Biochemistry Analysis

After 18 days of treatment, blood samples were collected after 12 h of fasting and centrifuged at 3000 rpm for 5 min to obtain the supernatant. Serum alanine aminotransferase (ALT), aspartate aminotransferase (AST), alkaline phosphatase (ALP), and lactic dehydrogenase (LDH) levels were measured using a biochemical analyzer (iMagic-V7, iCubio Biotech Company, Shenzhen, China).

## Liver Histology

At the end of treatment, histological analysis was performed to evaluate hepatocellular steatosis and fibrosis. For hematoxylin-eosin (H&E) staining, paraffin-embedded liver sections were incubated with H&E solutions (Servicebio, Wuhan, China). Paraffin-embedded sections were also stained with Sirius Red solution (Servicebio, Wuhan, China). Subsequently, sections were dehydrated with anhydrous ethanol and xylene and sealed with neutral gum. Frozen liver tissue slices were incubated with Oil Red solution (Servicebio, Wuhan, China) in the dark and immersed in hematoxylin for 3–5 min. The slices were then sealed with glycerin-gelatin. Histological assessment and scoring were performed by

a pathologist blinded to the study. The NAFLD Activity Scoring (NAS) (steatosis/inflammation/ballooning) were performed using the clinical criteria outlined by Kleiner et al.<sup>28</sup> Using Image J software to quantify the percentage of lipid droplet area and fibrosis positive area of the entire image area.

## Statistical Analyses

SigmaPlot software (version 12.5) was used to analyze all experimental data. The statistical analyses performed included the Student's *t*-test, one-way analysis of variance (ANOVA) and the Mann–Whitney test.  $p < 0.05$  indicated a statistically significant difference. The experimental data are expressed as mean  $\pm$  standard error of the mean (SEM).

## Results

### Identification of DEGs

Transcriptomic analysis was performed on small intestine tissues from the Control group, Model group and Geniposide group. DEGs were screened according to  $|\log_{2}FC| > 1$  and  $q\text{Value} < 0.05$ . Compared with the Control group, there were 721 DEGs in the Model group, including 170 upregulated genes and 551 downregulated genes. In the Geniposide group, there were 285 upregulated genes and 99 downregulated genes in comparison with the Model group. The volcano plots of DEGs are shown in [Figure 1A](#) and [B](#), respectively. Furthermore, 177 overlapping DEGs were found from Model vs Control (downregulated genes) and Geniposide vs Model (upregulated genes); 34 overlapping DEGs were found from Model vs Control (upregulated genes) and Geniposide vs Model (downregulated genes) ([Figure 1C](#) and [D](#)).

### The GLP-1R Agonist-Like Effects of Cinchonine Identified by CMap Analysis

The CMap database was used to screen candidate small-molecule drugs. We entered overlapping DEGs as a query signature in the CMap database and the top ten small-molecule drugs are listed in [Table 1](#). Cinchonine ranked first with a high connectivity score (enrichment score=0.911, mean=0.684), suggesting that cinchonine exerted GLP-1R agonist-like effects.

To evaluate the binding affinity of cinchonine and GLP-1R, molecular docking was performed using the SYBYL software. The results showed that cinchonine had a good binding affinity with GLP-1R (Total score=7.19; Cscore=4), and the amino acid residue-binding sites of cinchonine were A/GLU294 and A/GLN221 ([Figure 2](#)), suggesting that cinchonine is a potential GLP-1R agonist. However, further experimental verification is required.

### Cinchonine Promoted Insulin Secretion and Oral Administration of Cinchonine Reduced Blood Glucose in C57BL/6 Mice

Insulin deficiency is a critical pathogenesis of T2DM, and the effect of cinchonine on insulin secretion was investigated for the first time. The results showed that cinchonine significantly promoted insulin secretion at 11.1 mM glucose ([Figure 3A](#)). To examine the glucose-lowering effect of cinchonine by oral administration, C57BL/6 mice were single gavaged with various doses of cinchonine for performing OGTT. As shown in [Figure 3B](#), 100 and 200 mg/kg cinchonine significantly reduced blood glucose at 15 min, and the AUC was also significantly decreased compared with the mice gavaged with saline ([Figure 3C](#)). As 100 mg/kg cinchonine showed a good glucose-lowering effect, this dose was used in subsequent experiments.

### Cinchonine Promoted Insulin Secretion and Lowered Blood Glucose by Activating GLP-1R

A key benefit of GLP-1R agonists is glucose-dependent insulin secretion. Islets were exposed to cinchonine under different glucose concentrations (2.8, 11.1, 16.7 mM). As shown in [Figure 4A](#), cinchonine potentiated insulin secretion under high glucose conditions (11.1 and 16.7 mM) but had no effect under 2.8 mM glucose, which suggested that cinchonine induced insulin release in a glucose-dependent manner. Furthermore, Exendin (9–39), an antagonist of GLP-1R, was used to evaluate the effect of cinchonine on GLP-1R. As shown in [Figure 4B](#), the cinchonine-induced insulinotropic effect was weakened by Exendin (9–39).

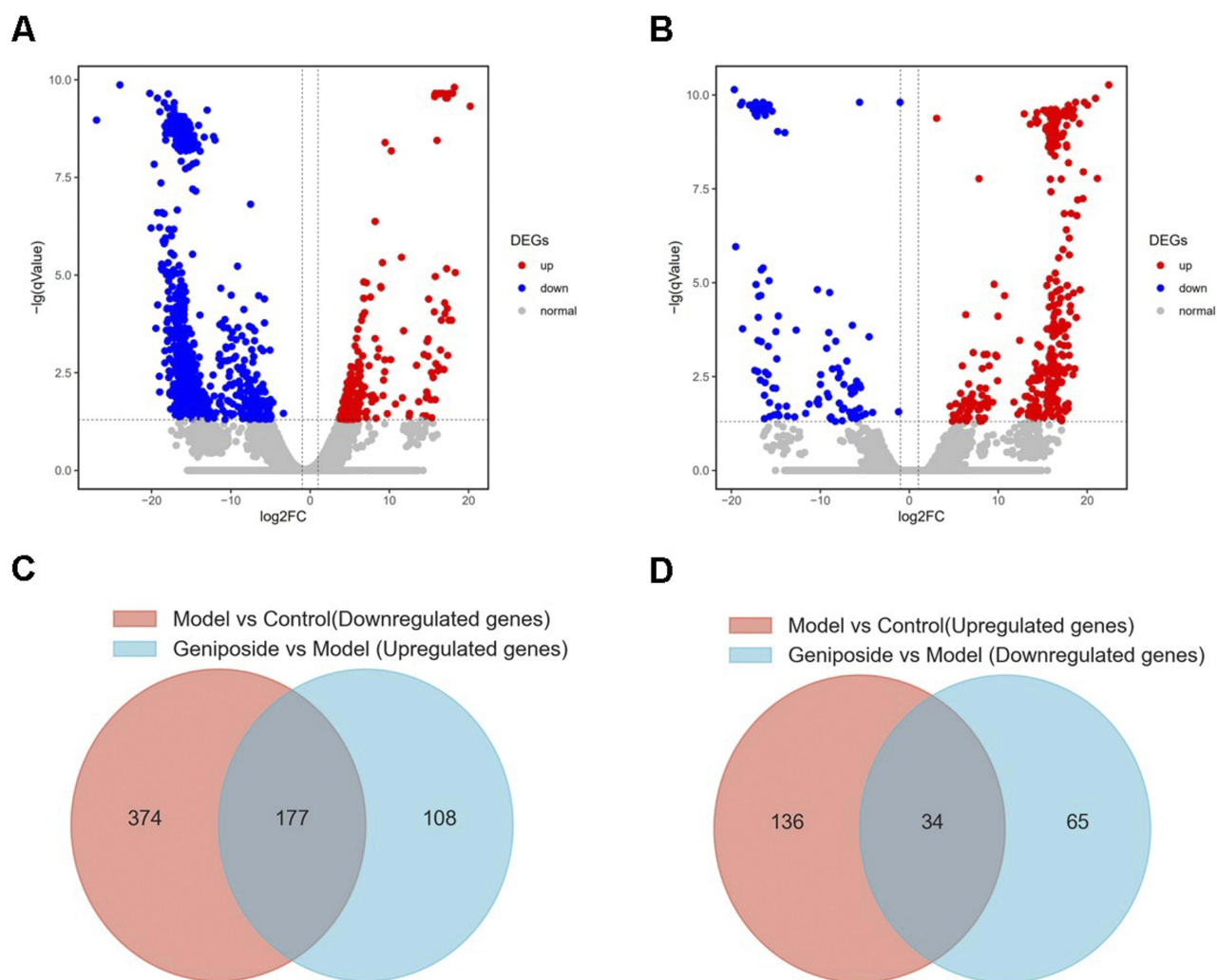


**Figure 1** Identification of differentially expressed genes (DEGs). **(A)** Volcano plot of the Model group compared with the Control group (Model vs Control). **(B)** Volcano plot of the Geniposide group compared with the Model group (Geniposide vs Model). Red and blue dots indicate upregulated and downregulated genes, respectively. **(C)** Venn diagram of overlapping DEGs in Model vs Control (downregulated genes) and Geniposide vs Model (upregulated genes). **(D)** Venn diagram of overlapping DEGs in Model vs Control (upregulated genes) and Geniposide vs Model (downregulated genes).

In addition, OGTT was performed using  $GLP-1R^{-/-}$  mice to confirm the activation of cinchonine on  $GLP-1R$ . As expected, the glucose-lowering effect of cinchonine was significantly weakened when  $GLP-1R$  was knocked out (Figure 4C and D). Moreover, we performed OGTT on  $hGLP-1R$  mice. The results indicated that cinchonine significantly

**Table 1** List the Top 10 Compounds of Connectivity Map

CMap Name	Mean	n	Enrichment	p
Cinchonine	0.684	4	0.911	0.00006
Biperiden	0.468	5	0.768	0.00148
Trimethadione	0.464	4	0.824	0.00151
Isometheptene	0.329	4	0.781	0.00434
Podophyllotoxin	0.496	4	0.775	0.00481
Gentamicin	0.436	4	0.773	0.00505
PF-00539745-00	0.599	3	0.855	0.00585
Gly-His-Lys	0.514	3	0.851	0.00619
Viomycin	0.443	4	0.761	0.00625
Carteolol	0.278	4	0.758	0.00647

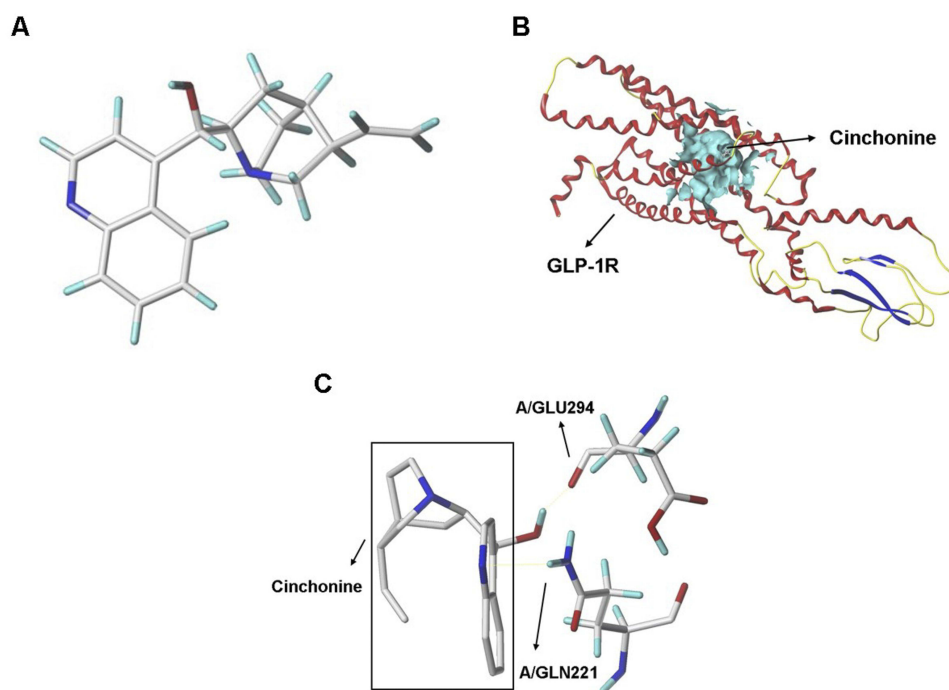


**Figure 2** Molecular docking shows that cinchonine has good binding affinity with GLP-1R. (A) Equilibrium structure of cinchonine. (B) Predicted binding sites of cinchonine on GLP-1R (PDB code: 5NX2). (C) Details of cinchonine binding to GLP-1R. The contact residues are labeled.

reduced blood glucose at 15 and 30 min, and the AUC was also significantly decreased compared with the mice gavaged with saline (Figure 4E and F).

### Oral Administration of Cinchonine Prevented Body Weight Gain and Inhibited Food Intake of ob/ob-GAN NASH Mice

To explore the effect of cinchonine on NASH, we fed the GAN diet to ob/ob mice. The results showed that the terminal body weight of ob/ob-GAN NASH mice increased to  $70.01 \pm 1.11$  g, equivalent to a gain of  $9.25 \pm 1.09\%$  relative to the initial weight. Cinchonine at 50 mg/kg ( $67.02 \pm 0.95$  g, body weight gain  $4.59 \pm 1.04\%$ ) slightly influenced weight gain. Whereas, cinchonine at 100 mg/kg ( $66.14 \pm 0.61$  g, body weight gain  $3.17 \pm 1.03\%$ ) significantly reduced body weight gain compared with Vehicle (Figure 5A and B). In addition, cinchonine had a dose-dependent effect on food intake reduction compared with Vehicle (Figure 5C).

### Oral Administration of Cinchonine Improved Liver Injury of Ob/Ob-GAN NASH Mice

As shown in Figure 6, the GAN diet led to a significant increase in serum ALT, AST, ALP, and LDH levels in ob/ob mice. 50 mg/kg cinchonine significantly attenuated ALP level. 100 mg/kg cinchonine significantly attenuated the levels of ALT, ALP, and LDH. However, the AST level was not decreased by cinchonine treatment.

### Oral Administration of Cinchonine Improved NAS Score of Ob/Ob-GAN NASH Mice

H&E staining (Figure 7A) showed an accumulation of fat droplets in the liver cells of ob/ob-GAN NASH mice compared with the NC group. Cinchonine dose-dependently alleviated GAN diet-induced liver steatosis. Moreover, the infiltration of inflammatory cells was observed in the liver of NASH mice, which was attenuated following the administration of cinchonine. NAS score, steatosis score, ballooning score and inflammation score of ob/ob-GAN NASH mice were significantly reduced after cinchonine treatment in a dose-dependent manner (Figure 7B-E). The results showed that cinchonine could reduce hepatic steatosis and protect liver injury.

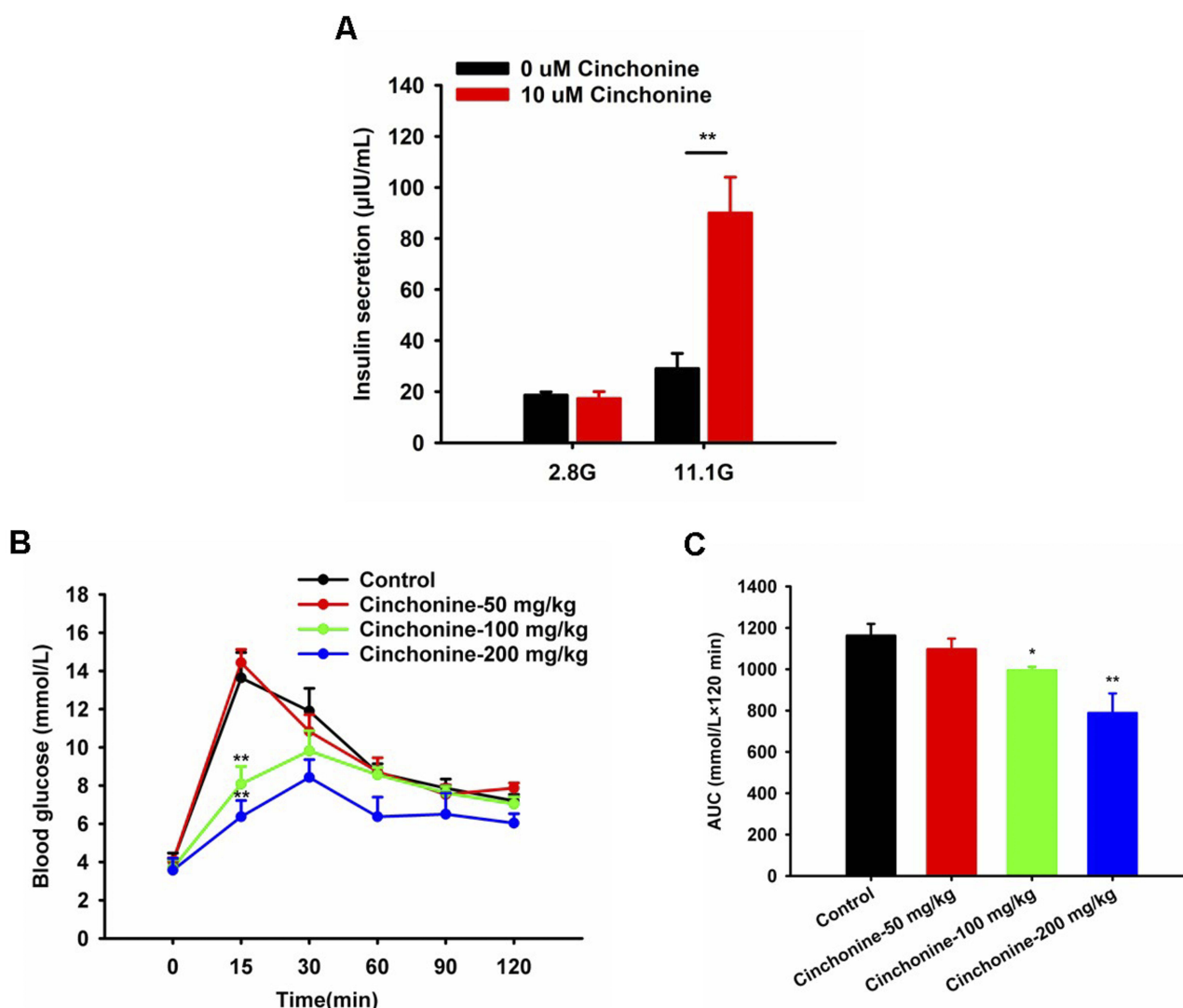


**Figure 3** Insulinotropic and glucose-lowering effects of cinchonine. **(A)** Treatment of islets with cinchonine (10  $\mu$ M) under 2.8 mM or 11.1 mM glucose ( $n=7$ ). **(B)** Oral glucose tolerance test (OGTT) was performed on C57BL/6 mice, and the area under the curve (AUC) was calculated **(C)** ( $n=3$ ). All experimental results are expressed as mean  $\pm$  SEM. Statistical differences in insulin secretion and blood glucose were obtained via one-way ANOVA or Student's *t*-test. Statistical differences in AUCs were evaluated using the Mann-Whitney Rank Sum test. \* $p<0.05$ , \*\* $p<0.01$ .

## Oral Administration of Cinchonine Ameliorated Hepatic Steatosis and Hepatic Fibrosis in Ob/Ob-GAN NASH Mice

To further assess the effect of cinchonine on hepatic steatosis, Oil Red O staining was performed. The liver cells showed large oil and small fat droplets were diffused in ob/ob-GAN NASH mice. Cinchonine dose-dependently reduced lipid droplets (Figure 8A). Oil red O lipid droplets positive area reduced compared to the Vehicle group (Figure 8B). The progression of NASH is closely related to the degree of liver fibrosis. We conducted Sirius red staining to assess the extent of fibrosis. As shown in Figure 8C, collagen deposition and clear fibrosis were observed in the liver tissues of NASH mice, which was significantly attenuated by cinchonine. Liver fibrosis positive area reduced compared to the Vehicle group (Figure 8D).

## Discussion

GLP-1R agonists are promising agents for treating type 2 diabetes mellitus that reduce blood glucose via glucose-dependent insulin secretion with minimized low risk of hypoglycaemia.<sup>29</sup> In addition, GLP-1R agonists decrease



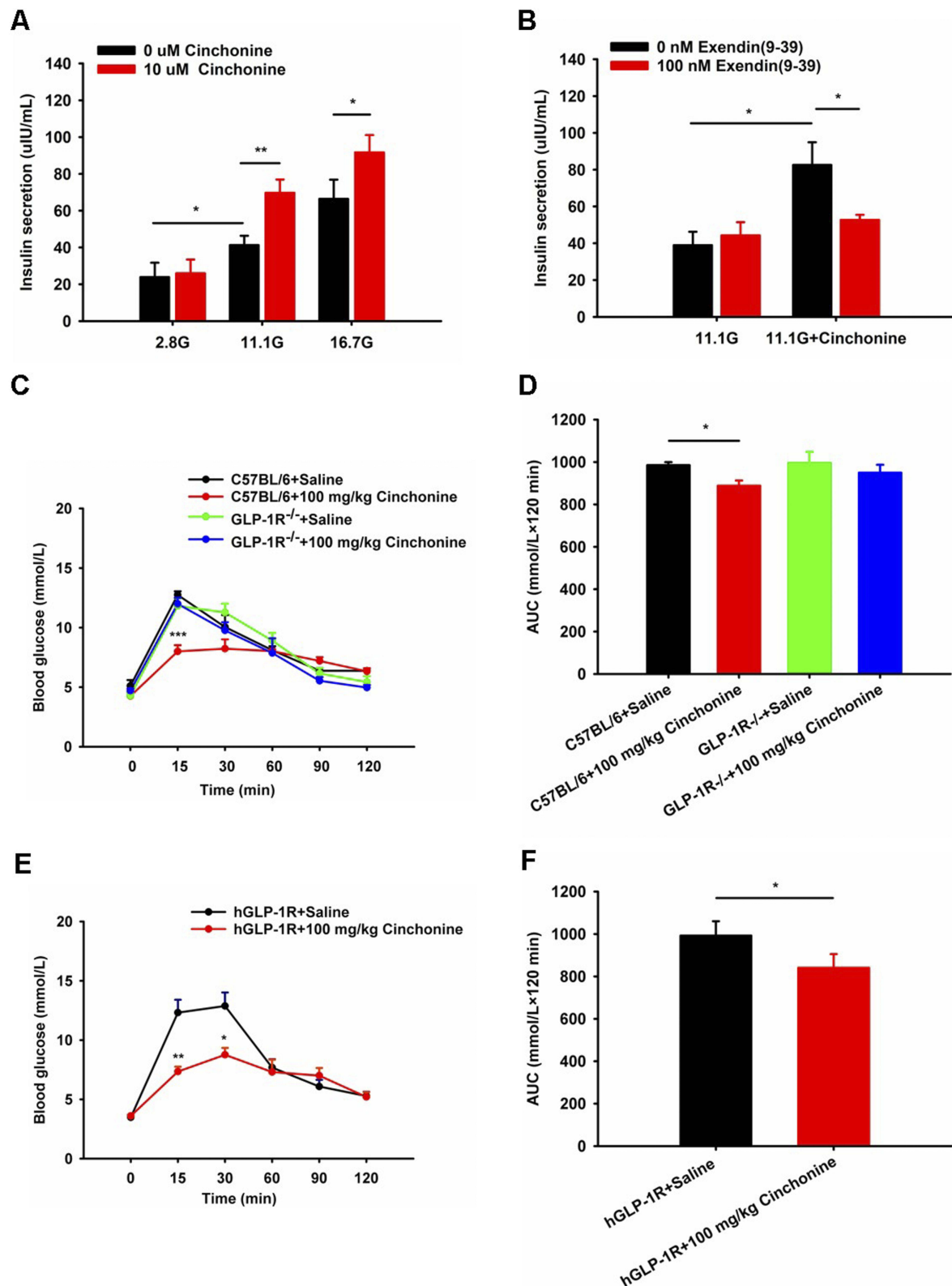


**Figure 4** Cinchonine exerts insulinotropic and glucose-lowering effects by activating GLP-1R. **(A)** Treating islets with cinchonine (10  $\mu$ M) under three glucose concentrations (2.8, 11.1, and 16.7 mM) revealed different levels of insulin secretion ( $n=7$ ). **(B)** Effect of Exendin (9–39) on insulin secretion induced by cinchonine ( $n=7$ ). **(C)** OGTT was performed on GLP-1R<sup>-/-</sup> mice, and AUC was calculated **(D)** ( $n=4$ ). **(E)** OGTT was performed in hGLP-1R mice, and AUC was calculated **(F)** ( $n=5$ ). All experimental results are expressed as mean  $\pm$  SEM. Statistical differences in insulin secretion and blood glucose were obtained by one-way ANOVA or Student's *t*-test. AUCs were compared using the Mann–Whitney Rank Sum test. \* $p<0.05$ , \*\* $p<0.01$ .

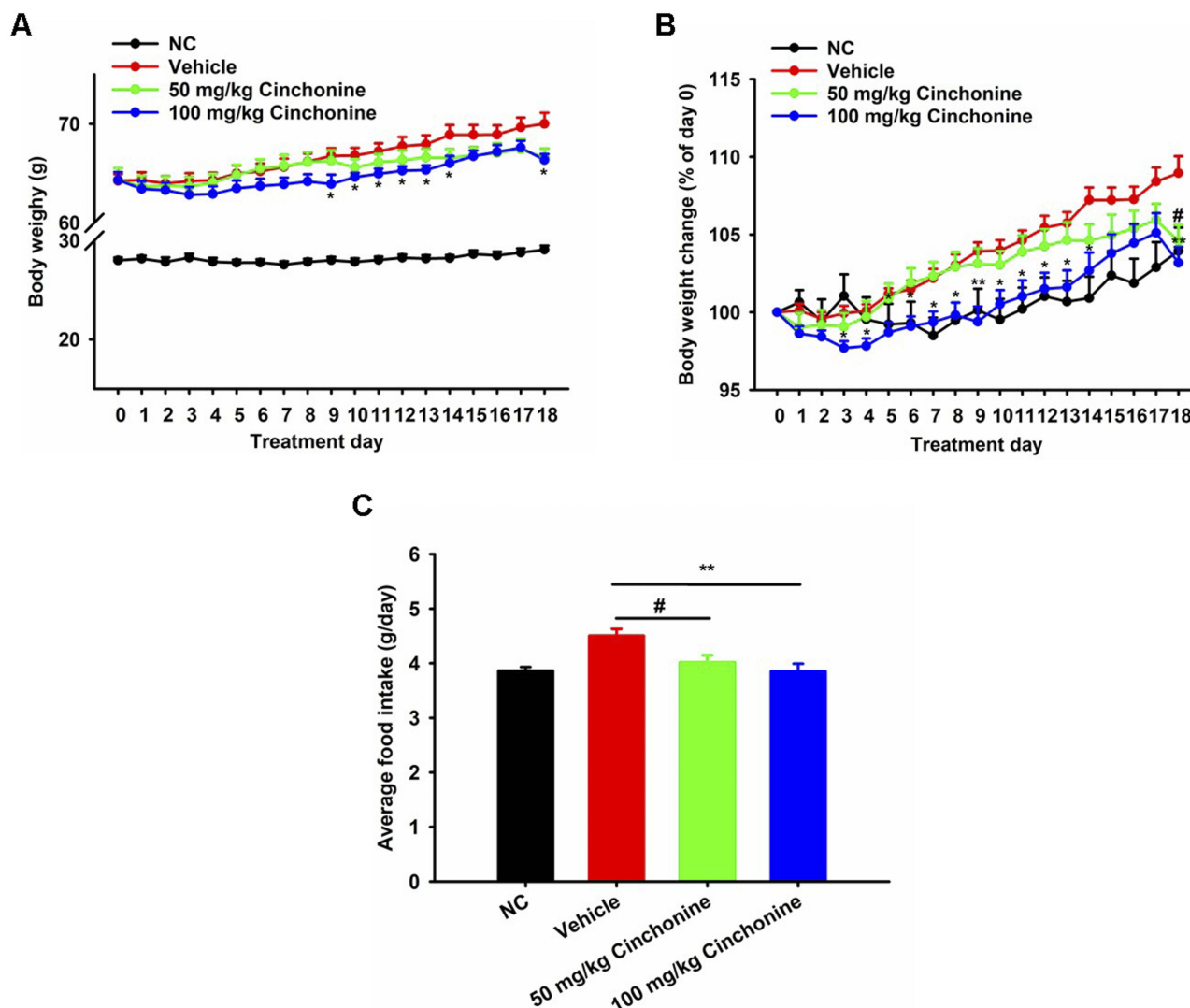


**Figure 5** Oral cinchonine treatment prevents body weight gain and food intake in ob/ob-GAN NASH mice (n=7). **(A)** Body weight (g). **(B)** Body weight change (% compared to initial body weight at the onset of cinchonine treatment). **(C)** Average food intake (g/day). All experimental results are expressed as mean  $\pm$  SEM. \* $p$ <0.05, \*\* $p$ <0.01, 100 mg/kg cinchonine compared with Vehicle; # $p$ <0.05, 50 mg/kg cinchonine compared with Vehicle.

glucagon secretion, decrease energy intake, prolong gastric emptying and increase satiety. However, GLP-1 peptide agonists currently administered by injection except for oral semaglutide, has stimulated the search for more convenient and orally administered drugs.<sup>30</sup> Hence, there is significant interest in the development of small-molecule GLP-1R agonists. In the present study, we attempt to screen for small-molecule GLP-1R agonists by CMap which is an online pharmacogenomic database links disease, genes and drugs by identifying similar or opposite gene expression profiles.

Geniposide, the main active ingredient of *Gardenia jasminoides* J.Ellis, has been reported to display various pharmacological activities, including anti-diabetes, anti-inflammation, and neuroprotection effects, by activating GLP-1R.<sup>31–37</sup> Our group constructed a gene expression profile database of GLP-1R agonists based on geniposide, which was used for treating db/db mice for 11 weeks. In the present study, we first analyzed the small intestine transcriptome of control vs model and geniposide vs model groups. These analyses revealed several overlapping DEGs, including 177 upregulated genes and 34 downregulated genes, which were linked to both the disease and the drug. Using the CMap database, we found that cinchonine presented the highest score indicating that this compound exerts GLP-1R agonist-like effects. In addition, molecular docking was used to identify drug targets, and a good binding affinity between cinchonine and GLP-1R was found. Collectively, these results suggest that cinchonine is a potential GLP-1R agonist.

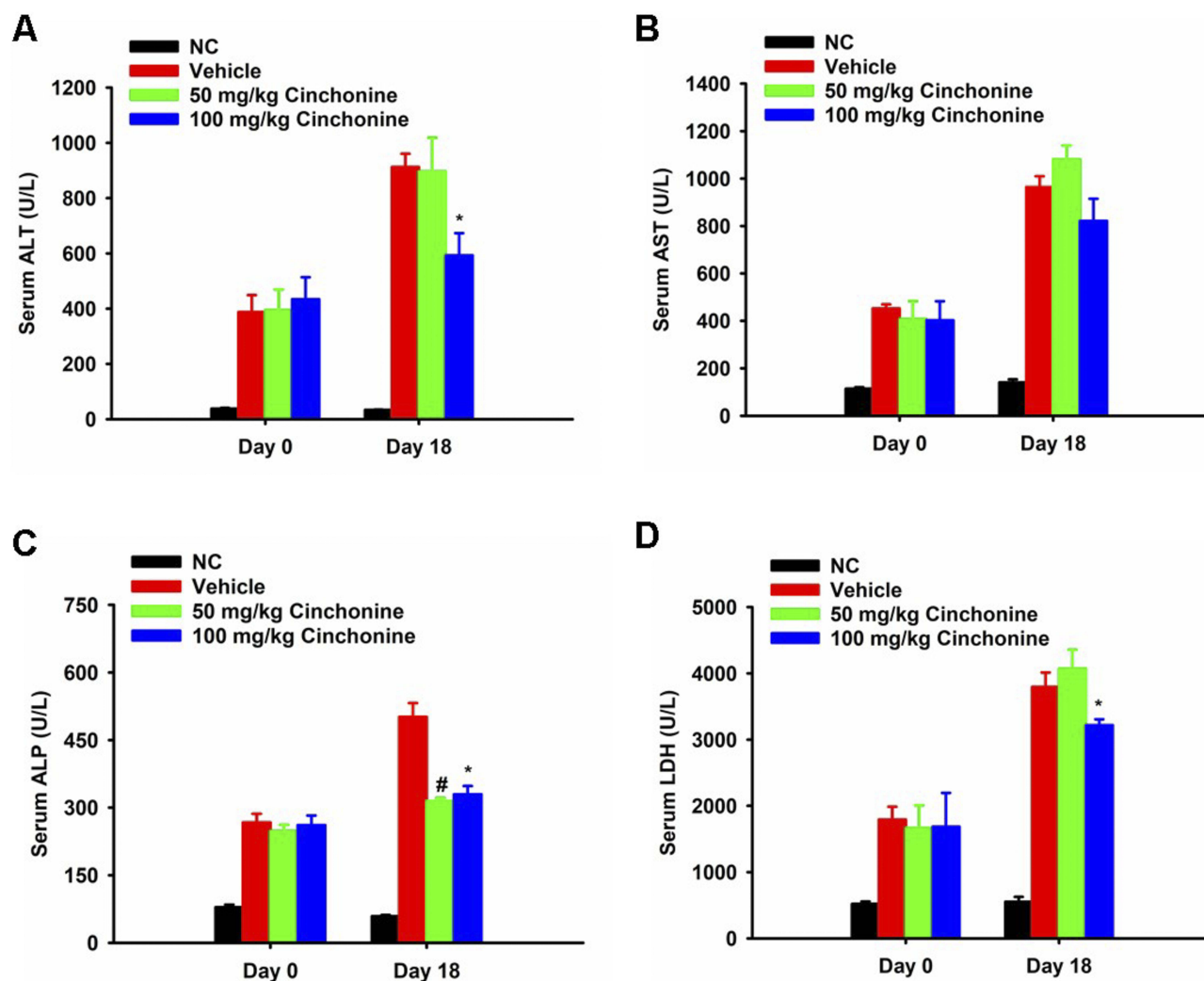


**Figure 6** Oral cinchonine treatment improves liver injury in ob/ob-GAN NASH mice (n=7). (A–D) Levels of serum alanine aminotransferase (ALT), aspartate aminotransferase (AST), alkaline phosphatase (ALP) and lactic dehydrogenase (LDH). Statistical differences were obtained using one-way ANOVA or Student's *t*-test. All experimental results are expressed as mean  $\pm$  SEM. \* $p$ <0.05, 100 mg/kg cinchonine compared with Vehicle; # $p$ <0.05, 50 mg/kg cinchonine compared with Vehicle.

GLP-1 is an incretin molecule mainly secreted by enteroendocrine L cells, alpha cells, and the central nervous system.<sup>38</sup> A key benefit of GLP-1R agonists is the glucose-dependent insulinotropic function, with reduction in blood glucose only in hyperglycemia, eliminating the hypoglycemia risk of many other antidiabetic drugs.<sup>39</sup> As expected, our results indicated that cinchonine promoted insulin secretion in a glucose-dependent manner. In addition, the cinchonine-induced insulin secretion was significantly reduced when GLP-1R was blocked with Exendin (9–39). Taken together, these two results confirm our initial hypothesis that cinchonine is a potential GLP-1R agonist.

To further explore the glucose-lowering effect of oral cinchonine, we conducted OGTT *in vivo*. In acute toxicity study, maximal tolerated *i.p.* dose of cinchonine was 200 mg/kg body in mice.<sup>40</sup> In addition, 0.05% dietary (equivalent to 50 mg/kg body weight) cinchonine prevents high-fat-diet-induced obesity of C57BL/6N mice.<sup>41</sup> Based on the results of previous studies, 50, 100 and 200 mg/kg cinchonine were used in OGTT. Our data showed that cinchonine significantly reduced blood glucose in C57BL/6 mice in a dose-dependent manner. On the other hand, this effect was significantly weakened in GLP-1R<sup>-/-</sup> mice, indicating that cinchonine is a potential orally available GLP-1R agonist. Moreover, we revealed that cinchonine could also reduce blood glucose of hGLP-1R mice, suggesting cinchonine may be useful in humans and providing a basis for its clinical application in the future.

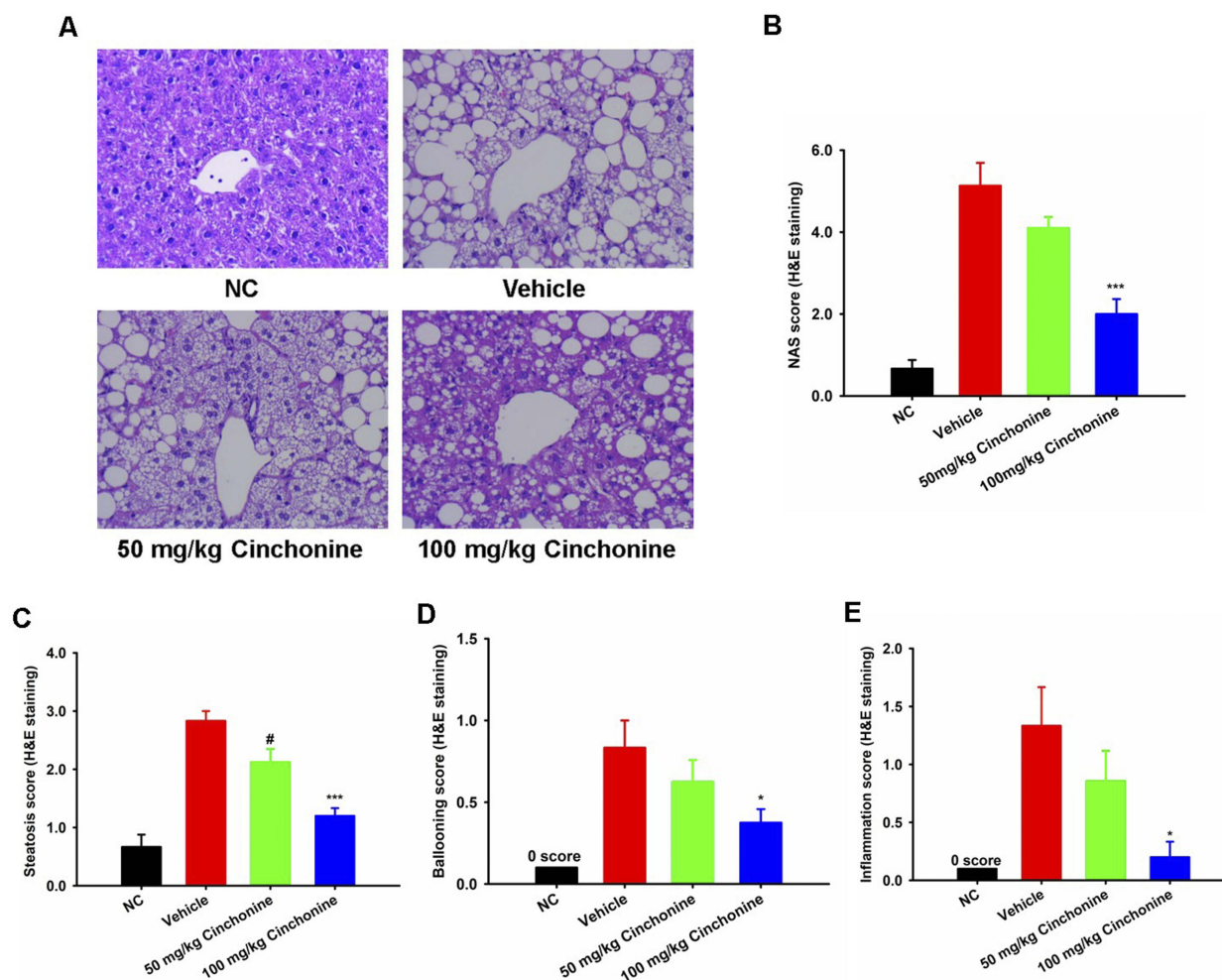


**Figure 7** Oral cinchonine treatment improves NAFLD Activity Scoring (NAS) in ob/ob-GAN NASH mice (n=7). **(A)** Representative histology of H&E staining (Scale bar, 50  $\mu$ m). **(B)** NAS score. **(C-E)** Histological analysis of steatosis, ballooning and inflammation. Statistical differences were obtained using one-way ANOVA or Student's *t*-test. All experimental results are expressed as mean  $\pm$  SEM. \* $p$ <0.05, \*\*\* $p$ <0.001, 100 mg/kg cinchonine compared with Vehicle; # $p$ <0.05, 50 mg/kg cinchonine compared with Vehicle.

Additionally, NASH is a serious liver disease for which there are no approved drugs. GLP-1R agonists are important candidate for the treatment of NASH.<sup>42,43</sup> Several GLP-1R agonists, including exenatide, liraglutide, and semaglutide, have been used in NASH clinical research.<sup>44,45</sup> Therefore, we conducted a study to evaluate the effect of cinchonine on NASH. Although there are many modeling methods for NASH, the ob/ob-GAN NASH model is similar to human NASH characteristics of obesity and prominent liver fibrosis.<sup>46,47</sup> Thus, we fed ob/ob mice with the GAN diet to construct the NASH model in the present study.

After GAN-diet feeding, the body weight and food intake of the ob/ob mice increased significantly. The levels of serum ALT, AST, ALP, and LDH were also markedly elevated. In addition, severe liver steatosis lipid droplets were observed in liver cells using H&E and Oil Red O staining. The progression of NASH is closely related to the degree of liver fibrosis,<sup>48</sup> and hepatic collagen deposition and fibrosis was observed by Sirius Red staining, suggesting that we successfully established a NASH model. In our study, we noted that liver fibrosis occurred in ob/ob mice fed the GAN diet, owing to the older age of ob/ob mice (25 weeks) and the long duration of their obesity.

Weight loss is linked to reduced hepatic steatosis.<sup>49</sup> Preclinical and clinical studies using GLP-1R agonists demonstrate that reductions in hepatic steatosis, inflammation, and liver injury are generally associated with weight loss.<sup>50,51</sup> As expected, cinchonine dose-dependently reduced body weight gain in ob/ob-GAN NASH mice, which was consistent with decreased food intake. In addition, 100 mg/kg cinchonine significantly improved liver function by reducing the ALT,

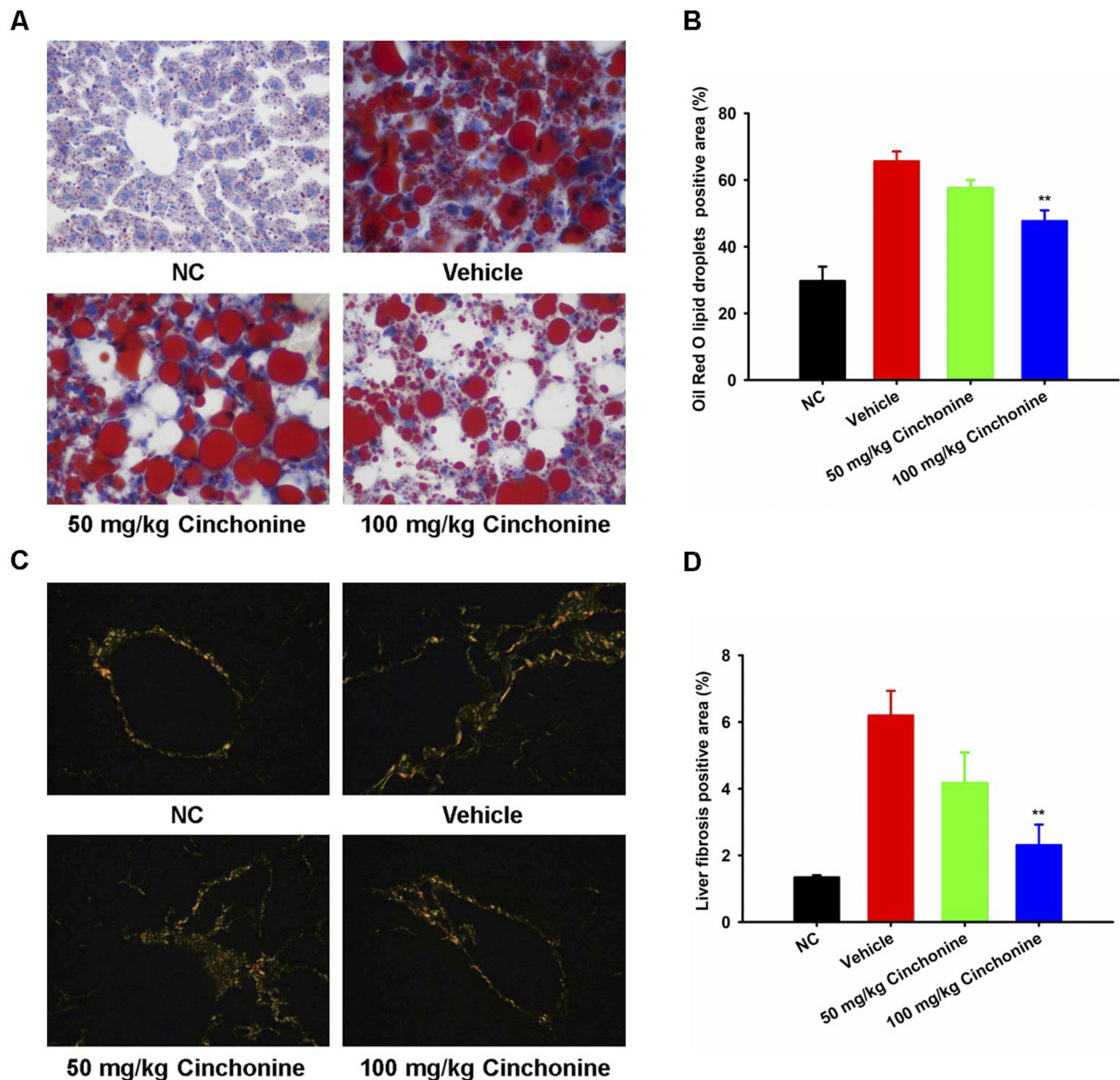


**Figure 8** Oral cinchonine ameliorates hepatic steatosis and hepatic fibrosis in ob/ob-GAN NASH mice (n=7). (**A** and **C**) Representative histology of Oil Red O staining and Sirius Red staining in liver tissues (Scale bar, 50  $\mu$ m). (**B** and **D**) Quantification of positive staining areas were measured by Image J software. Statistical differences were obtained using one-way ANOVA or Student's *t*-test. All experimental results are expressed as mean  $\pm$  SEM. \*\**p*<0.01, 100 mg/kg cinchonine compared with Vehicle.

ALP, and LDH levels. Importantly, 100 mg/kg cinchonine was found to ameliorate hepatic steatosis and hepatic fibrosis in NASH mice.

In addition to its antimalarial effect, cinchonine has been reported to inhibit human platelet aggregation via reducing calcium ion influx and inhibiting the protein kinase C pathway in platelets.<sup>52,53</sup> In addition, cinchonine can inhibit toll-like receptor 2- (TLR2-) and TLR4-mediated signaling cascades, and attenuate pro-inflammatory cytokine levels in high-fat diet-induced obesity mice.<sup>41</sup> Cinchonine was also recently reported to induce apoptosis of HeLa and A549 cells by inhibiting transforming growth factor- $\beta$ -activated kinase 1 and protein kinase B through binding to tumor necrosis factor receptor associated factor 6.<sup>54</sup> Therefore, although we found that cinchonine lowered blood glucose and ameliorated NASH by activating GLP-1R, it cannot be excluded that it has other mechanisms to enhance or attenuate these effects.

## Conclusions

In conclusion, this study demonstrated that cinchonine, as a potential oral small-molecule GLP-1R agonist, reduces blood glucose and ameliorates NASH. Our findings confirm the importance of drug repurposing for the discovery of GLP-1R agonists. Although further exploration is needed, the discovery of cinchonine still provides feasible methods and ideas for the development of small-molecule GLP-1R agonists.

## Ethics Approval and Consent to Participate

The animal study protocol was approved by the Laboratory Animal Ethical Committee of Shanxi Medical University. The use of animals conformed to the Guide for the Care and Use of Laboratory Animals of Shanxi Medical University (GBT 35892-2018).

## Funding

This research was funded by the NSFC (No. 81973378 and 82073909), Basic Research Plan in Shanxi Province of China (No. 202103021223219 and 20210302124584), FSKSC, and 1331KSC.

## Disclosure

The authors declare no conflicts of interest.

## References

1. Cloete L. Diabetes mellitus: an overview of the types, symptoms, complications and management. *Nurs Stand*. 2022;37(1):61–66. doi:10.7748/ns.2021.e11709
2. Magliano DJ, Boyko EJ. *IDF DIABETES ATLAS*. 10th ed. Brussels; 2021.
3. Nauck MA, Quast DR, Wefers J, Meier JJ. GLP-1 receptor agonists in the treatment of type 2 diabetes-state-of-the-art. *Mol Metab*. 2021;46:101102. doi:10.1016/j.molmet.2020.101102
4. Andersen A, Lund A, Knop FK, Vilsboll T. Glucagon-like peptide 1 in health and disease. *Nat Rev Endocrinol*. 2018;14(7):390–403. doi:10.1038/s41574-018-0016-2
5. Zhao X, Wang M, Wen Z, et al. GLP-1 Receptor Agonists: beyond Their Pancreatic Effects. *Front Endocrinol (Lausanne)*. 2021;12:721135. doi:10.3389/fendo.2021.721135
6. Dokmak A, Lizaola-Mayo B, Trivedi HD. The Impact of Nonalcoholic Fatty Liver Disease in Primary Care: a Population Health Perspective. *Am J Med*. 2021;134(1):23–29. doi:10.1016/j.amjmed.2020.08.010
7. Korinkova L, Prazienkova V, Cerna L, et al. Pathophysiology of NAFLD and NASH in Experimental Models: the Role of Food Intake Regulating Peptides. *Front Endocrinol (Lausanne)*. 2020;11:597583. doi:10.3389/fendo.2020.597583
8. Siddiqui MS, Harrison SA, Abdelmalek MF, et al. Case definitions for inclusion and analysis of endpoints in clinical trials for nonalcoholic steatohepatitis through the lens of regulatory science. *Hepatology*. 2018;67(5):2001–2012. doi:10.1002/hep.29607
9. Sharma D, Verma S, Vaidya S, Kalia K, Tiwari V. Recent updates on GLP-1 agonists: current advancements & challenges. *Biomed Pharmacother*. 2018;108:952–962. doi:10.1016/j.biopha.2018.08.088
10. Hirsch IB. The Future of the GLP-1 Receptor Agonists. *JAMA*. 2019;321(15):1457–1458. doi:10.1001/jama.2019.2941
11. Miyasaka K. New drug for type 2 diabetes: introduction of oral Semaglutide (Rybelsus(R)) tablets, an oral GLP-1 receptor agonist. *Nihon Yakurigaku Zasshi*. 2022;157(2):146–154. doi:10.1254/fpj.21052
12. Pratley R, Amod A, Hoff ST, et al. investigators P. Oral semaglutide versus subcutaneous liraglutide and placebo in type 2 diabetes (PIONEER 4): a randomised, double-blind, phase 3a trial. *Lancet*. 2019;394(10192):39–50. doi:10.1016/S0140-6736(19)31271-1
13. Mendez M, Matter H, Defossa E, et al. Design, Synthesis, and Pharmacological Evaluation of Potent Positive Allosteric Modulators of the Glucagon-like Peptide-1 Receptor (GLP-1R). *J Med Chem*. 2020;63(5):2292–2307. doi:10.1021/acs.jmedchem.9b01071
14. Zhao P, Liang Y-L, Belousoff MJ, et al. Activation of the GLP-1 receptor by a non-peptidic agonist. *Nature*. 2020;577(7790):432–436. doi:10.1038/s41586-019-1902-z
15. Saxena AR, Gorman DN, Esquejo RM, et al. Danuglipron (PF-06882961) in type 2 diabetes: a randomized, placebo-controlled, multiple ascending-dose Phase 1 trial. *Nat Med*. 2021;27(6):1079–1087. doi:10.1038/s41591-021-01391-w
16. Pushpakom S, Iorio F, Eyers PA, et al. Drug repurposing: progress, challenges and recommendations. *Nat Rev Drug Discov*. 2019;18(1):41–58. doi:10.1038/nrd.2018.168
17. Sonaye HV, Sheikh RY, Doifode CA. Drug repurposing: iron in the fire for older drugs. *Biomed Pharmacother*. 2021;141:111638. doi:10.1016/j.biopha.2021.111638
18. Parvathaneni V, Kulkarni NS, Muth A, Gupta V. Drug repurposing: a promising tool to accelerate the drug discovery process. *Drug Discov Today*. 2019;24(10):2076–2085. doi:10.1016/j.drudis.2019.06.014
19. Qu XA, Rajpal DK. Applications of Connectivity Map in drug discovery and development. *Drug Discov Today*. 2012;17(23–24):1289–1298. doi:10.1016/j.drudis.2012.07.017
20. Xiao SJ, Zhu XC, Deng H, et al. Gene expression profiling coupled with Connectivity Map database mining reveals potential therapeutic drugs for Hirschsprung disease. *J Pediatr Surg*. 2018;53(9):1716–1721. doi:10.1016/j.jpedsurg.2018.02.060

21. Luo S, Li H, Mo Z, et al. Connectivity map identifies luteolin as a treatment option of ischemic stroke by inhibiting MMP9 and activation of the PI3K/Akt signaling pathway. *Exp Mol Med.* 2019;51(3):1–11. doi:10.1038/s12276-019-0229-z
22. Sowunmi A, Salako LA, Laoye OJ, Aderounmu AF. Combination of quinine, quinidine and cinchonine for the treatment of acute falciparum malaria: correlation with the susceptibility of Plasmodium falciparum to the cinchona alkaloids in vitro. *Trans R Soc Trop Med Hyg.* 1990;84(5):626–629. doi:10.1016/0035-9203(90)90127-z
23. Boratynski PJ, Zielinska-Blajet M, Skarzewski J. Cinchona Alkaloids-Derivatives and Applications. *Alkaloids Chem Biol.* 2019;82:29–145. doi:10.1016/bs.alkal.2018.11.001
24. Lamb J, Crawford ED, Peck D, et al. The Connectivity Map: using gene-expression signatures to connect small molecules, genes, and disease. *Science.* 2006;313(5795):1929–1935. doi:10.1126/science.1132939
25. Joshi SD, Dixit SR, Kirankumar MN, et al. Synthesis, antimycobacterial screening and ligand-based molecular docking studies on novel pyrrole derivatives bearing pyrazoline, isoxazole and phenyl thiourea moieties. *Eur J Med Chem.* 2016;107:133–152. doi:10.1016/j.ejmech.2015.10.047
26. Liu Z, Yang H, Zhi L, et al. Sphingosine 1-phosphate Stimulates Insulin Secretion and Improves Cell Survival by Blocking Voltage-dependent K(+) Channels in beta Cells. *Front Pharmacol.* 2021;12:683674. doi:10.3389/fphar.2021.683674
27. Liu T, Cui L, Xue H, et al. Telmisartan Potentiates Insulin Secretion via Ion Channels, Independent of the AT1 Receptor and PPARgamma. *Front Pharmacol.* 2021;12:739637. doi:10.3389/fphar.2021.739637
28. Kleiner DE, Brunt EM, Van Natta M, et al. Design and validation of a histological scoring system for nonalcoholic fatty liver disease. *Hepatology.* 2005;41(6):1313–1321. doi:10.1002/hep.20701
29. Nadkarni P, Chepurny OG, Holz GG. Regulation of glucose homeostasis by GLP-1. *Prog Mol Biol Transl Sci.* 2014;121:23–65. doi:10.1016/B978-0-12-800101-1.00002-8
30. Zhang X, Belousoff MJ, Zhao P, et al. Differential GLP-1R Binding and Activation by Peptide and Non-peptide Agonists. *Mol Cell.* 2020;80(3):485–500e487. doi:10.1016/j.molcel.2020.09.020
31. Zhang Y, Ding Y, Zhong X. Geniposide acutely stimulates insulin secretion in pancreatic beta-cells by regulating GLP-1 receptor/cAMP signaling and ion channels. *Mol Cell Endocrinol.* 2016;430:89–96. doi:10.1016/j.mce.2016.04.020
32. Liu J, Zheng X, Yin F, et al. Neurotrophic property of geniposide for inducing the neuronal differentiation of PC12 cells. *Int J Dev Neurosci.* 2006;24(7):419–424. doi:10.1016/j.ijdevneu.2006.08.009
33. Zheng Y, Xiao Y, Zhang D, et al. Geniposide Ameliorates Dexamethasone-Induced Cholesterol Accumulation in Osteoblasts by Mediating the GLP-1R/ABCA1 Axis. *Cells.* 2021;10:12. doi:10.3390/cells10123424
34. Zhao Y, Li H, Fang F, et al. Geniposide improves repeated restraint stress-induced depression-like behavior in mice by ameliorating neuronal apoptosis via regulating GLP-1R/AKT signaling pathway. *Neurosci Lett.* 2018;676:19–26. doi:10.1016/j.neulet.2018.04.010
35. Liu J, Guo L, Yin F, Zhang Y, Liu Z, Wang Y. Geniposide regulates glucose-stimulated insulin secretion possibly through controlling glucose metabolism in INS-1 cells. *PLoS One.* 2013;8(10):e78315. doi:10.1371/journal.pone.0078315
36. Guo LX, Xia ZN, Gao X, Yin F, Liu JH. Glucagon-like peptide 1 receptor plays a critical role in geniposide-regulated insulin secretion in INS-1 cells. *Acta Pharmacol Sin.* 2012;33(2):237–241. doi:10.1038/aps.2011.146
37. Liu J, Yin F, Xiao H, Guo L, Gao X. Glucagon-like peptide 1 receptor plays an essential role in geniposide attenuating lipotoxicity-induced beta-cell apoptosis. *Toxicol In Vitro.* 2012;26(7):1093–1097. doi:10.1016/j.tiv.2012.07.004
38. Graaf C, Donnelly D, Wootten D, et al. Glucagon-Like Peptide-1 and Its Class B G Protein-Coupled Receptors: a Long March to Therapeutic Successes. *Pharmacol Rev.* 2016;68(4):954–1013. doi:10.1124/pr.115.011395
39. Lu JM. The Role of Glucagon-Like Peptide-1 Receptor Agonists in Type 2 Diabetes in Asia. *Adv Ther.* 2019;36(4):798–805. doi:10.1007/s12325-019-00914-9
40. Genne P, Dimanche-Boitrel MT, Mauvernay RY, et al. Cinchonine, a potent efflux inhibitor to circumvent anthracycline resistance in vivo. *Cancer Res.* 1992;52(10):2797–2801.
41. Jung SA, Choi M, Kim S, Yu R, Park T. Cinchonine Prevents High-Fat-Diet-Induced Obesity through Downregulation of Adipogenesis and Adipose Inflammation. *PPAR Res.* 2012;2012:541204. doi:10.1155/2012/541204
42. Imajo K, Fujita K, Yoneda M, et al. Hyperresponsivity to low-dose endotoxin during progression to nonalcoholic steatohepatitis is regulated by leptin-mediated signaling. *Cell Metab.* 2012;16(1):44–54. doi:10.1016/j.cmet.2012.05.012
43. Clarke JD, Dzierlenga AL, Nelson NR, et al. Mechanism of Altered Metformin Distribution in Nonalcoholic Steatohepatitis. *Diabetes.* 2015;64(9):3305–3313. doi:10.2337/db14-1947
44. Younossi ZM, Loomba R, Rinella ME, et al. Current and future therapeutic regimens for nonalcoholic fatty liver disease and nonalcoholic steatohepatitis. *Hepatology.* 2018;68(1):361–371. doi:10.1002/hep.29724
45. Mantovani A, Byrne CD, Targher G. Efficacy of peroxisome proliferator-activated receptor agonists, glucagon-like peptide-1 receptor agonists, or sodium-glucose cotransporter-2 inhibitors for treatment of non-alcoholic fatty liver disease: a systematic review. *Lancet Gastroenterol Hepatol.* 2022;7(4):367–378. doi:10.1016/S2468-1253(21)00261-2
46. Hansen HH. Human translatability of the GAN diet-induced obese mouse model of non-alcoholic steatohepatitis. *BMC Gastroenterol.* 2020;20(1):210. doi:10.1186/s12876-020-01356-2
47. Boland ML, Oro D, Tolbol KS, et al. Towards a standard diet-induced and biopsy-confirmed mouse model of non-alcoholic steatohepatitis: impact of dietary fat source. *World J Gastroenterol.* 2019;25(33):4904–4920. doi:10.3748/wjg.v25.i33.4904
48. Kumar S, Duan Q, Wu R, Harris EN, Su Q. Pathophysiological communication between hepatocytes and non-parenchymal cells in liver injury from NAFLD to liver fibrosis. *Adv Drug Deliv Rev.* 2021;176:113869. doi:10.1016/j.addr.2021.113869
49. Pan CS, Stanley TL. Effect of Weight Loss Medications on Hepatic Steatosis and Steatohepatitis: a Systematic Review. *Front Endocrinol (Lausanne).* 2020;11:70. doi:10.3389/fendo.2020.00070
50. Newsome PN, Buchholtz K, Cusi K, et al. Trial of Subcutaneous Semaglutide in Nonalcoholic Steatohepatitis. *N Engl J Med.* 2021;384(12):1113–1124. doi:10.1056/NEJMoa2028395
51. Perakakis N, Stefanakis K, Feigh M, Veidal SS, Mantzoros CS. Elafibranor and liraglutide improve differentially liver health and metabolism in a mouse model of non-alcoholic steatohepatitis. *Liver Int.* 2021;41(8):1853–1866. doi:10.1111/liv.14888
52. Shah BH, Safdar B, Virani SS, Nawaz Z, Saeed SA, Gilani AH. The antiplatelet aggregatory activity of Acacia nilotica is due to blockade of calcium influx through membrane calcium channels. *Gen Pharmacol.* 1997;29(2):251–255. doi:10.1016/s0306-3623(96)00413-2

53. Shah BH, Nawaz Z, Virani SS, Ali IQ, Saeed SA, Gilani AH. The inhibitory effect of cinchonine on human platelet aggregation due to blockade of calcium influx. *Biochem Pharmacol.* 1998;56(8):955–960. doi:10.1016/s0006-2952(98)00094-x
54. Qi Y, Pradipta AR, Li M, et al. Cinchonine induces apoptosis of HeLa and A549 cells through targeting TRAF6. *J Exp Clin Cancer Res.* 2017;36(1):35. doi:10.1186/s13046-017-0502-8

Drug Design, Development and Therapy

Dovepress

## Publish your work in this journal

Drug Design, Development and Therapy is an international, peer-reviewed open-access journal that spans the spectrum of drug design and development through to clinical applications. Clinical outcomes, patient safety, and programs for the development and effective, safe, and sustained use of medicines are a feature of the journal, which has also been accepted for indexing on PubMed Central. The manuscript management system is completely online and includes a very quick and fair peer-review system, which is all easy to use. Visit <http://www.dovepress.com/testimonials.php> to read real quotes from published authors.

Submit your manuscript here: <https://www.dovepress.com/drug-design-development-and-therapy-journal>